Available online at www.sciencedirect.com
ScienceDirect
International Journal of Heat and Fluid Flow 27 (2006) 800–810
International Journal of HEAT AND FLUID FLOW
www.elsevier.com/locate/ijhff

LES, T-RANS and hybrid simulations of thermal convection at high *Ra* numbers

S. Kenjereš *, K. Hanjalić

Department of Multi Scale Physics, Faculty of Applied Sciences, Delft University of Technology, Lorentzweg 1, 2628 CJ Delft, The Netherlands

Received 3 October 2005; received in revised form 29 January 2006; accepted 4 March 2006
Available online 15 June 2006

Abstract

The paper reports on application of different approaches to the simulations of thermal convection at high Rayleigh (*Ra*) numbers. Based on new well-resolved LES in $10^7 \leqslant Ra \leqslant 10^9$ range, the performance of a T-RANS (using a low-*Re* three-equation $\langle k\rangle$–$\langle\varepsilon\rangle$–$\langle\theta^2\rangle$ ASM/AFM subscale model) and a hybrid approach (utilizing the concept of "seamless" RANS/LES merging) have been compared. Targeting accurate predictions of heat transfer at very high *Ra* numbers, the near-wall behaviour of the subscale turbulence contributions is analyzed in details. Whilst the application of the conventional LES on a coarse grid resulted in huge underprediction of the Nusselt number (50% at $Ra = 10^9$), thanks to a well-tuned subscale model, the T-RANS results showed excellent agreement for heat transfer with both the fine-resolved LES (for $Ra \leqslant 10^9$) and experimental data for over a ten-decades range of *Ra* ($10^6 \leqslant Ra \leqslant 2 \times 10^{16}$). The visible absence of the fine-scale motion in the T-RANS, however, means that the T-RANS will perform poorly in flows where there are no strong large-scale forcing, as, e.g., in a side-heated vertical channel. In order to sensitize the T-RANS approach to high-frequency instabilities, different ways of hybrid RANS/LES merging based on "seamless" approach have been investigated. It is demonstrated that the hybrid approach is capable of capturing a significantly larger portion of the fine-structure spectrum than is possible with T-RANS, whilst also returning accurate predictions of heat transfer and turbulence statistics.

Keywords: Numerical simulations; Turbulent thermal convection; High resolution LES; T-RANS; Hybrid RANS/LES

1. Introduction

Most industrial and environmental flows driven by buoyancy (crystal growth, reactor safety, indoor- and outdoor climate control, cooling of electronics) occur at very high Rayleigh numbers ($Ra > 10^{10}$). For such applications, the direct and large-eddy simulation techniques, DNS and LES, become prohibitively expensive (see, e.g., Hanjalić, 2005). The upper limit for DNS is at present $Ra \approx 10^8$ (van Reeuwijk et al., submitted for publication), but most results available in the literature deal with one or two decades lower *Ra*'s (Grötzbach, 1983; Wörner, 1994; Kerr, 1996; Kerr and Herring, 2000; Hartlep et al., 2003). The LES can reach somewhat higher *Ra*, though again the published results do not go beyond 10^9 (Eidson, 1985; Wong and Lilly, 1994; Kimmel and Domaradzki, 2000). Complex flow domains pose additional challenge for DNS and LES, often requiring sophisticated grid design, clustering and local refinement. But most of all, the orientation of the imposed temperature gradient with respect to the gravitational vector can have a dramatic influence on the character of the underlying physics, posing different demands on simulations. A case in focus is the thermal convection between two parallel infinite plates heated differentially: the horizontal orientation produces very different flow and turbulent structure from the vertical one even at the same *Ra* number. These two configurations have, therefore, been considered as "a must" for testing the generality of any statistical turbulence models.

The horizontal fluid layers heated from bellow, corresponding to the classic Rayleigh–Bénard (R–B) convection,

* Corresponding author. Tel.: +31 15 2783649; fax: +31 15 2781204.
E-mail address: kenjeres@ws.tn.tudelft.nl (S. Kenjereš).

0142-727X/$ - see front matter © 2006 Elsevier Inc. All rights reserved.
doi:10.1016/j.ijheatfluidflow.2006.03.008

Nomenclature

$Ra = \beta g_i \Delta T Pr \left(\frac{\rho}{\mu}\right)^2 D^3$	Rayleigh number
$Nu = \frac{hD}{\lambda}$	Nusselt number
$Re_t = \frac{\langle k\rangle^2}{\nu\langle\varepsilon\rangle}$	Reynolds turbulent number
$Pr = \frac{\nu}{a}$	Prandtl number
$\langle U_i\rangle$	velocity vector (m/s)
$\langle T\rangle$	temperature (K)
$\langle k\rangle$	turbulent kinetic energy (m^2/s^2)
R	time scale ratio (–)
ΔT	wall temperature difference (K)
z_W	wall-distance (m)
g_i	gravitational vector (m/s^2)
$C_\theta, \ldots, C_\mu$	constants in turbulence model

Greek symbols

α	model parameter
β	thermal expansion coefficient (1/K)
β^*	model parameter
ρ	fluid density (kg/m^3)
ν	kinematic viscosity (m^2/s)
ν_t	turbulent viscosity (m^2/s)
ξ, η	constants in turbulence model
κ	von Karman constant
$\langle\theta^2\rangle$	temperature variance (K^2)
$\langle\varepsilon\rangle$	dissipation rate of turbulent kinetic energy (m^2/s^3)
$\langle\varepsilon_\theta\rangle$	dissipation rate of temperature variance (K^2/s)
$\langle\varepsilon_{\theta i}\rangle$	molecular dissipation rate of heat flux (m K/s^2)
$\mathscr{T}$	mechanical time scale (s)
$\mathscr{T}_\theta$	thermal time scale (s)
τ_{ij}	subscale/subgrid stress (m^2/s^2)
$\tau_{\theta i}$	subscale/subgrid turbulent heat flux (m K/s)

are especially challenging for simulation because of high demand for numerical resolution of the wall boundary layers, which becomes progressively thinner with an increase in the *Ra* number. The application of the standard wall-functions with RANS or LES is known to produce very erroneous heat transfer coefficient (Nusselt numbers), leaving the integration up to the wall as the only choice for accurate predictions of wall phenomena. In addition to accurate predictions, industrial applications require a fast and numerically robust approach which will make parameterization studies possible. On the other hand, the R–B convection is dominated by large-scale convective roll-cell structures, which provide very strong forcing, thus making this flow tractable by different types of very large-eddy simulation (VLES) techniques, such as transient-RANS (T-RANS) and others. These methods usually do not work in flows with a broader turbulence spectrum, such as found in the same channel configuration, but oriented vertically. This is the main motivation for exploring some novel hybrid RANS/LES approaches, which should capture at least the (very) large-scale turbulence fluctuations and provide some spectral information.

In this paper we compare the fine-resolved LES, T-RANS and hybrid approaches to the simulation of R–B convection. Because of grid resolution problem with conventional LES for high *Ra* and *Re* numbers and still large uncertainties in RANS for thermal convection, we focus on combining the best features of RANS (satisfactory near-wall predictions using a RANS-type grid) and LES (proper spatial and time resolution of turbulence structures away from a solid wall). Because the well-resolved reliable DNS or LES results for thermal convection are scarce in the literature and limited (at present) to low values of *Ra* ($\leqslant 10^8$), we first performed a series of well-resolved LES in $10^7 \leqslant Ra \leqslant 10^9$ range. After that we investigated possibilities for merging RANS and LES methods by employing hybrid "seamless" approach. Comparative assessment of LES (both well resolved and coarse), T-RANS and hybrid method is performed focusing on the wall-heat transfer and different subscale/subgrid contributions to second-moments.

2. Equations and subscale/subgrid turbulence models

The conservation equations for momentum and energy for buoyancy driven incompressible fluid flow (with Boussinesq approximation) can be written as

$$\frac{\mathrm{D}\langle U_i\rangle}{\mathrm{D}t} = \frac{\partial}{\partial x_j}\left(\nu\frac{\partial\langle U_i\rangle}{\partial x_j} - \tau_{ij}\right) - \frac{1}{\rho}\frac{\partial(\langle P\rangle - P_{\mathrm{REF}})}{\partial x_i} - \beta g_i(\langle T\rangle - T_{\mathrm{REF}}) \tag{1}$$

$$\frac{\mathrm{D}\langle T\rangle}{\mathrm{D}t} = \frac{\partial}{\partial x_j}\left(\frac{\nu}{Pr}\frac{\partial\langle T\rangle}{\partial x_j} - \tau_{\theta j}\right) \tag{2}$$

where $\langle\,\rangle$ stands for Reynolds (time or ensemble) averaged quantities in RANS and spatially filtered quantities in LES. The turbulent stress (τ_{ij}) and heat flux ($\tau_{\theta i}$) represent the unresolved turbulence contributions – on subgrid or subscale levels for LES and T-RANS approach, respectively. In order to close the system of equations, these contributions must be modelled. In the present work, we adopted the well tested and tuned three-equations $\langle k\rangle$–$\langle\varepsilon\rangle$–$\langle\theta^2\rangle$ ASM/AFM model for the T-RANS approach, Kenjereš and Hanjalić (1999, 2002). For the subgrid contributions for LES we adopted the buoyancy extended Smagorinsky (1983) model of Eidson (1985). The hybrid approach is based on the "seamless" coupling between the T-RANS (in the near-wall region) and LES (in the rest of the flow) by applying an approach based on the proposal of Dejoan and Schiestel (2001). A short overview of all models used is given next.

Table 1
Subscale T-RANS model coefficients

C_θ	$C_{\varepsilon 1}$	$C_{\varepsilon 2}$	C_μ	$C_{\varepsilon\theta i}$	ξ	η	R
0.2	1.44	1.92	0.09	7×10^{-4}	0.6	0.6	0.5

2.1. Subscale model for T-RANS

In order to properly capture the near-wall behaviour of turbulence quantities, the low-Reynolds (integration up to the wall) three-equation model is used, Kenjereš and Hanjalić (1999, 2002). The turbulent stress and heat flux are expressed via a "reduced-algebraic" truncation of their parent differential equations, while retaining all source terms:

$$\tau_{ij} = \frac{2}{3}\langle k\rangle\delta_{ij} - \nu_t\left(\frac{\partial\langle U_i\rangle}{\partial x_j} + \frac{\partial\langle U_j\rangle}{\partial x_i}\right) + C_\theta\beta\left(g_i\tau_{\theta j} + g_j\tau_{\theta i} - \frac{2}{3}g_k\tau_{\theta k}\delta_{ij}\right)\mathscr{T} \quad (3)$$

$$\tau_{\theta i} = -C_\theta\left(\tau_{ij}\frac{\partial\langle T\rangle}{\partial x_j} + \xi\tau_{\theta j}\frac{\partial\langle U_i\rangle}{\partial x_j} + \eta\beta g_i\langle\theta^2\rangle + \langle\varepsilon_{\theta i}\rangle\right)\mathscr{T} \quad (4)$$

The system is fully closed with three-additional equations for remaining turbulence quantities:

$$\frac{\mathrm{D}\langle k\rangle}{\mathrm{D}t} = \mathscr{D}_k - \tau_{ij}\frac{\partial\langle U_i\rangle}{\partial x_j} - \beta g_i\tau_{\theta i} - \langle\varepsilon\rangle \quad (5)$$

$$\frac{\mathrm{D}\langle\theta^2\rangle}{\mathrm{D}t} = \mathscr{D}_\theta - 2\tau_{\theta j}\frac{\langle\partial T\rangle}{\partial x_j} - 2\langle\varepsilon_\theta\rangle \quad (6)$$

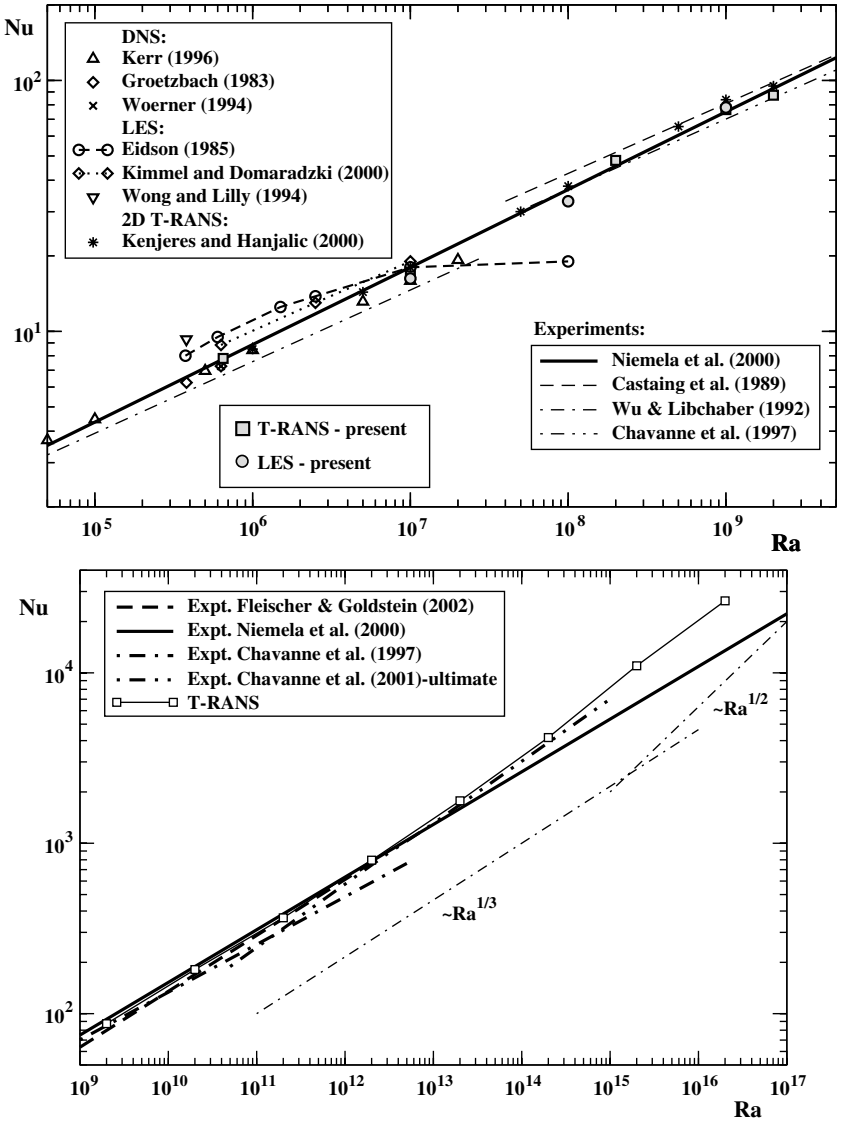

Fig. 1. Comparison of the computed $Nu(Ra)$ results with several DNS, LES and experimental correlations for a turbulent thermal convection of air over flat horizontal walls. Above: in intermediate range of Ra ($6.5\times10^5 \leqslant Ra \leqslant 2\times10^9$). Below: for high Ra range including ultra-turbulent regime ($2\times10^{10} \leqslant Ra \leqslant 2\times10^{16}$).

$$\frac{\mathrm{D}\langle\varepsilon\rangle}{\mathrm{D}t} = \mathscr{D}_\varepsilon - \frac{1}{\mathscr{T}}\left[C_{\varepsilon 1}\left(\tau_{ij}\frac{\partial\langle U_i\rangle}{\partial x_j} + \beta g_i \tau_{\theta i}\right) + C_{\varepsilon 2} f_\varepsilon \langle\varepsilon\rangle\right] + 2\nu\nu_\mathrm{t}\left(\frac{\partial^2\langle U_i\rangle}{\partial x_j \partial x_k}\right)^2 + S_l \tag{7}$$

$$\nu_\mathrm{t} = C_\mu f_\mu \langle k\rangle \mathscr{T} \tag{8}$$

where $\mathscr{T} = \langle k\rangle/\langle\varepsilon\rangle$ is the characteristic time scale while $f_\mu = \exp[-3.4/(1 + Re_\mathrm{t}/50)^2]$ and $f_\varepsilon = 1 - 0.3\exp(-Re_\mathrm{t}^2)$ are low-Re damping functions. These damping functions are based on the local turbulence parameters instead of the local wall-distances which makes them more appropriate for complex geometries, and Re_t is turbulent Reynolds number defined as $Re_\mathrm{t} = \langle k\rangle^2/\nu\langle\varepsilon\rangle$. Instead of solving an additional equation for the dissipation of the temperature variance $\langle\varepsilon_\theta\rangle$, the constant thermal-to-mechanical turbulence time scale ratio is assumed, i.e., $R = \mathscr{T}/\mathscr{T}_\theta = \langle\theta^2\rangle\langle\varepsilon\rangle/\langle k\rangle\langle\varepsilon_\theta\rangle = \text{const}$. The molecular heat flux dissipation term is represented in following form:

$$\langle\varepsilon_{\theta i}\rangle = f_{\varepsilon\theta i}\frac{1 + Pr}{2\sqrt{PrR}}\frac{\langle\varepsilon\rangle}{\langle k\rangle}\tau_{\theta i} \tag{9}$$

with $f_{\varepsilon\theta i} = \exp[-C_{\varepsilon\theta i} Re_\mathrm{t}(1 + Pr)]$, as proposed in Wörner and Grötzbach (1995). The S_l term in $\langle\varepsilon\rangle$ equation is length-scale correction term expressed as

$$S_l = \max\left[0.83\frac{\langle\varepsilon\rangle^2}{\langle k\rangle}\left(\frac{\langle k\rangle^{3/2}}{2.5\langle\varepsilon\rangle x_n} - 1\right)\left(\frac{\langle k\rangle^{3/2}}{2.5\langle\varepsilon\rangle x_n}\right)^2, 0\right] \tag{10}$$

All coefficients of the subscale T-RANS model are given in Table 1.

2.2. Subgrid model for LES

The LES subgrid model is based on the simple eddy-viscosity Smagorinsky formulation with an extension that includes buoyancy production effects – as proposed by Eidson (1985):

$$\nu_\mathrm{t}^\mathrm{SGS} = C\Delta^2\left(|S|^2 + \frac{\beta g_i}{Pr_\mathrm{t}}\frac{\partial\langle T\rangle}{\partial x_i}\right)^{1/2}, \tag{11}$$

$$\alpha_\mathrm{t}^\mathrm{SGS} = \frac{C}{Pr_\mathrm{t}}\Delta^2\left(|S|^2 + \frac{\beta g_i}{Pr_\mathrm{t}}\frac{\partial\langle T\rangle}{\partial x_i}\right)^{1/2} \tag{12}$$

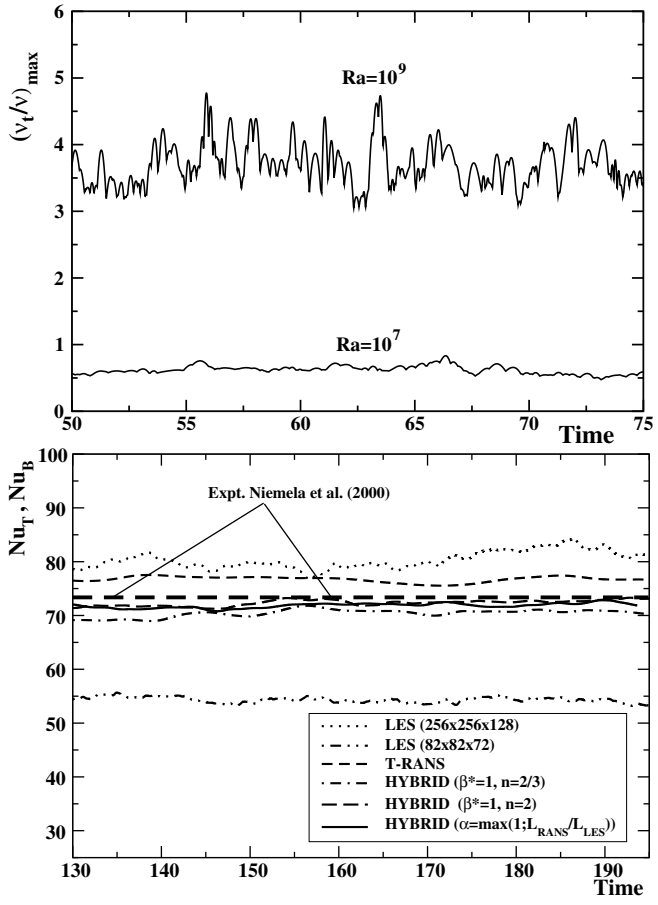

Fig. 2. Above: ratio between turbulent and molecular viscosity for different values of Ra (10^7, 10^9) – the well-resolved $256^2 \times 128$ LES. Below: time evolution of overall Nusselt number at horizontal walls – comparison between experimental, well resolved and coarse LES, T-RANS and HYBRID approach (with different values of β^* and n as well as with the α parameter).

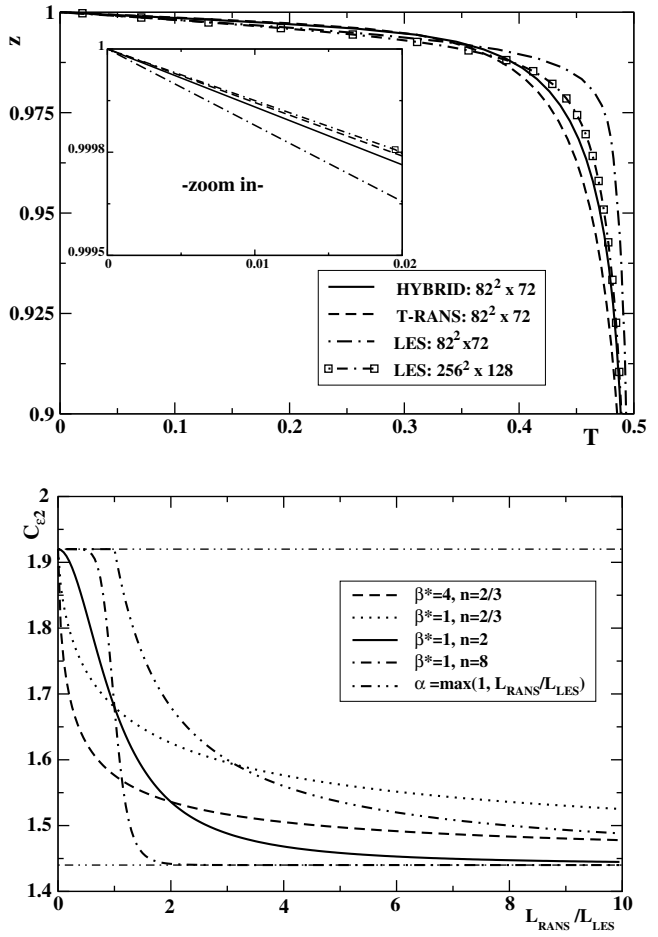

Fig. 3. Above: long-term averaged vertical temperature profiles in proximity of the top wall ($1 \leqslant z/D \leqslant 0.9$) – LES, T-RANS and HYBRID results. Below: dependence of $C_{\varepsilon 2}$ coefficient on ratio between RANS and LES turbulence length scales for different values of β^* and n.

where $C = 0.01$ and $Pr_t = 0.4$ are the subgrid model coefficients, $|S| = (2S_{ij}S_{ij})^{1/2}$ is the modulus of the strain rate ($S_{ij} = 1/2(\partial\langle U_i\rangle/\partial x_j + \partial\langle U_j\rangle/\partial x_i)$), and $\Delta = (\Delta x\Delta y\Delta z)^{1/3} = (\Delta\mathrm{Vol})^{1/3}$ is characteristic filter length. It is noted that this formulation implies the representation of the subgrid heat flux via the simple-gradient-diffusion-hypothesis (SGDH), i.e., $\tau_{\theta i} = -\nu_t^{SGS}/Pr_t\partial\langle T\rangle/\partial x_i$.

2.3. Hybrid RANS/LES: "seamless" approach

In the present work we adopted the "seamless" hybrid approach based on the work of Dejoan and Schiestel (2001) and Schiestel and Dejoan (2005). This method uses a single RANS model to provide the eddy viscosity for the unresolved/subscale turbulence in the complete flow domain. Here the RANS model is the above defined three-equations model and the only difference is in the redefinition of the coefficient $C_{\varepsilon 2}$ in the equation for the dissipation of turbulence kinetic energy $\langle\varepsilon\rangle$. Two variants are considered:

- Dejoan and Schiestel (2001):

$$C_{\varepsilon 2} = C_{\varepsilon 1} + \frac{0.48}{1 + \beta^*\left(\frac{L_{RANS}}{L_{LES}}\right)^n} \tag{13}$$

- the new model:

$$C_{\varepsilon 2} = C_{\varepsilon 1} + \frac{0.48}{\alpha} \tag{14}$$

where $L_{RANS} = \kappa z_W$ and $L_{LES} = (\Delta\mathrm{Vol})^{1/3}$ are the RANS and LES length scales – respectively, and β^* and n are empirical constants that need to be determined, Dejoan and Schiestel (2001). In order to further reduce the empirical input into the "seamless" approach and to make the method more suitable for the complex geometries, we introduced the parameter $\alpha = \max(1, L_{RANS}/L_{LES})$ with $L_{RANS} = f_\mu\langle k\rangle^{3/2}/\langle\varepsilon\rangle$, Eq. (14).

3. Numerical method

The discretized equation set is solved using a structured finite-volume Navier–Stokes solver for three-dimensional

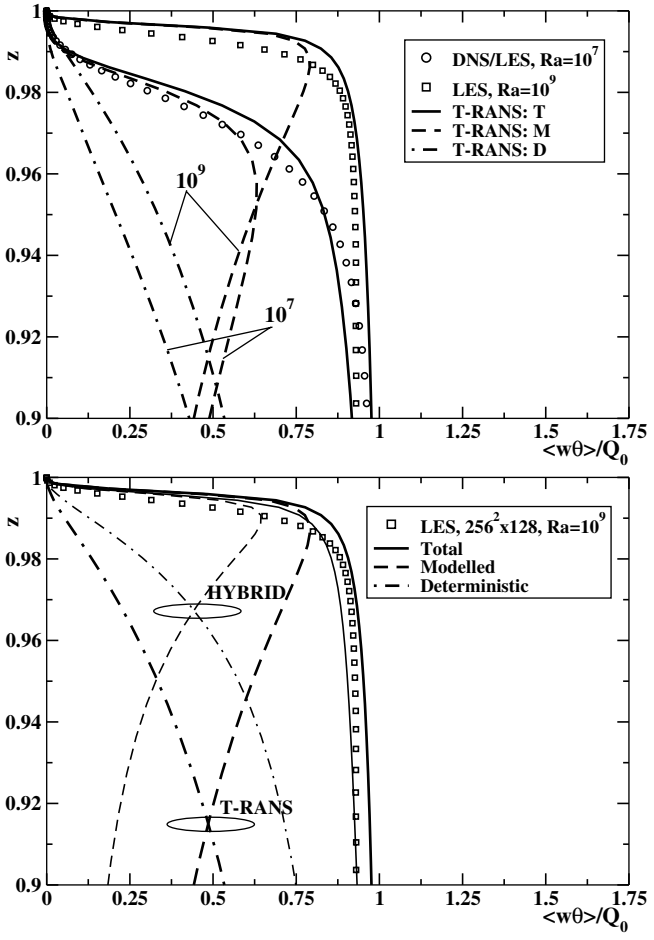

Fig. 4. Long-term averaged vertical turbulent heat flux profiles. Above: DNS/LES, LES and T-RANS comparison for $10^7 \leqslant Ra \leqslant 10^9$. Below: modelled (M), deterministic (D) and total (T) contributions in T-RANS and HYBRID approach for $Ra = 10^9$.

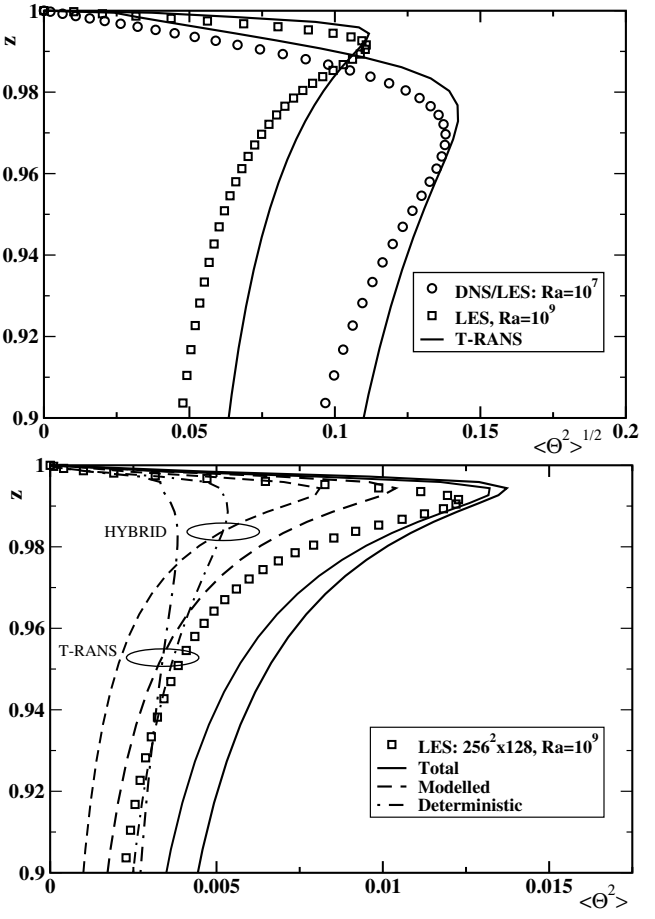

Fig. 5. Long-term averaged vertical temperature variance profiles. Above: DNS/LES, LES and T-RANS comparison for $10^7 \leqslant Ra \leqslant 10^9$. Below: modelled (M), deterministic (D) and total (T) contributions in T-RANS and HYBRID approach for $Ra = 10^9$.

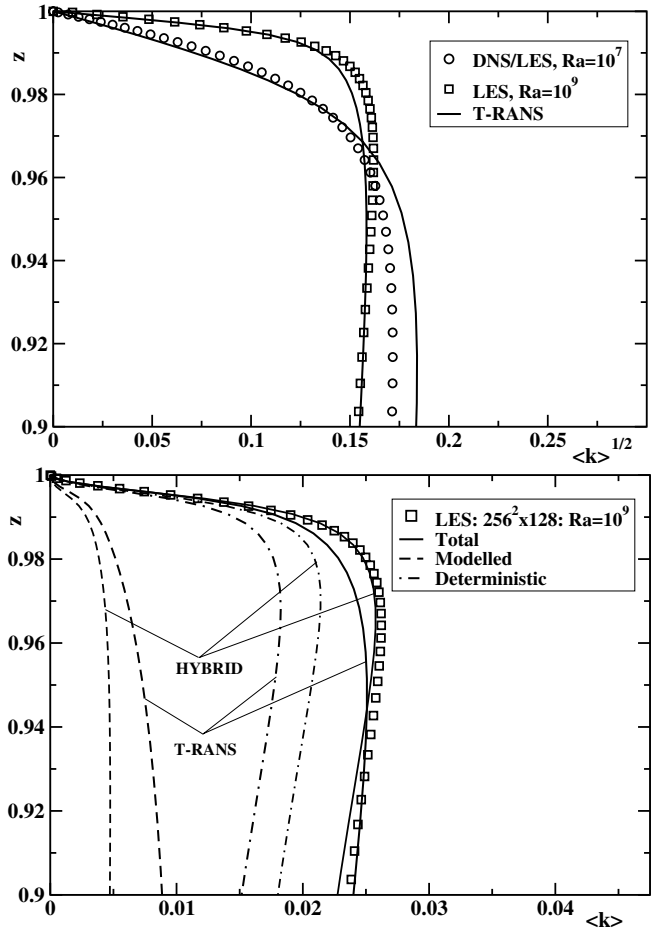

Fig. 6. Long-term averaged turbulence kinetic energy profiles. Left: DNS/LES, LES and T-RANS comparison for $10^7 \leqslant Ra \leqslant 10^9$. Right: modelled (M), deterministic (D) and total (T) contributions in T-RANS and HYBRID approach for $Ra = 10^9$.

flows, applicable to general non-orthogonal geometries. The Cartesian vectors and tensors components in the collocated grid arrangements are applied for all variables. The SIMPLE algorithm is used for coupling between the velocity and pressure fields. The second-order central difference scheme (CDS) is applied for the discretization of the diffusive terms in all equations and of convective terms in $\langle U, V, W, T\rangle$ equations (T-RANS, LES and HYBRID approach). The second-order linear upwind scheme (LUDS) is applied for convective terms in subscale turbulence equations, i.e., $\langle k, \varepsilon, \theta^2\rangle$. The time integration is performed by fully implicit second-order three-time-levels method which allows larger time steps to be used as compared to explicit time marching integration. The solver can be run in serial (single processor) or parallel mode utilizing the domain decomposition MPI directives. For the latter, the number of CPUs varied from 8 (for T-RANS, HYBRID and coarse-LES studies) to 64 (for fine-LES simulations) always resulting in an ideal speed-up on the SGI Origin 3800 platform.[1]

[1] SARA Computing and Networking Services, Amsterdam, The Netherlands; www.sara.nl.

4. Results

As mentioned in the introduction, we performed first a series of well-resolved LES of thermal convection between two flat horizontal walls with aspect ratio (4:4:1) heated from below and cooled from above in the range of high Ra numbers (up to $Ra = 10^9$) – all for $Pr = 0.71$ – an extension by one order of magnitude in Ra compared with (at the present) the highest Ra reached by the DNS of van Reeuwijk et al. (submitted for publication) and almost two order of magnitude higher than the DNS of Kerr (1996) and Kerr and Herring (2000). The side boundaries are treated as free-slip in order to have identical specification of boundary conditions as in DNS of Kerr and Herring (2000). The buoyancy extended version of the Smagorinsky formulation is used as the SGS model, Eidson (1985). The grid resolution was $256^2 \times 128$ control volumes – with the thickness of the first control volume next to the wall of $\Delta z_W = 2.5 \times 10^{-4}$ and 10^{-4}, which should ensure proper resolving of the wall thermal boundary layers. The typical values of the non-dimensional time step was $\Delta t = t\sqrt{\beta g \Delta T / H} = 5 \times 10^{-3}$ and 10^{-3} for $Ra = 10^7$ and 10^9, respectively. The simulations produced good agreement with the available experimental (Castaing et al., 1989; Wu and Libchaber, 1992; Chavanne et al., 1997; Niemela et al., 2000; Fleischer and Goldstein, 2002), DNS (for $Ra = 10^7$) (Grötzbach, 1983; Wörner, 1994; Kerr, 1996; Kerr and Herring, 2000) and T-RANS results (Kenjereš and Hanjalić, 1999, 2000, 2002) – in terms of the integral heat transfer (Nusselt number), Fig. 1(above). This is not surprising since the numerical grid was fine enough to fully resolve all scales (both spatially and in time) at $Ra = 10^7$ – producing practically a DNS. For $Ra = 10^9$ we made additional grid refinement with denser clustering towards the wall and we claim that we have a well-resolved LES up to the wall. The sufficiency of the spatial and temporal numerical resolution is illustrated in Fig. 2(above) showing the time evolution of the maximum value of the ratio between the turbulent and molecular viscosity.

Application of a conventional LES to higher values of Ra is seriously questioned. A simple analysis based on the ratio between the dissipation length scale and the distance between the walls shows that an immense grid resolution is needed for fully resolved simulations, e.g., for $Ra = 10^{14}$ and 10^{17} – DNS will require 3.5×10^4 and 2.5×10^5 grid points in the vertical direction, Kerr (1996). Adding to this the limits associated with the time step and the need to perform the time integration over at least a few convective time scales – one can conclude that at present (even when using massively parallel systems and optimistic prognosis) the upper affordable limit of DNS is $Ra \approx 10^{10}$. With the same massive computer resources, LES can possibly reach one more decade in Ra number. In order to overcome this problem, a possibility of merging RANS and LES approaches is investigated next. The goal of this merging is to find a proper method which will make

possible to provide accurate heat transfer prediction in complex geometries while employing affordable – moderately dense (RANS-type) – numerical grids.

In our previous works, Kenjereš and Hanjalić (1999, 2000, 2002) and Hanjalić and Kenjereš (2001a,b, 2002a,b), reported on the potential of the transient-RANS (T-RANS) approach to satisfactorily predict heat transfer in similar configurations by resolving in time and space the large convective structures and using the single-point RANS three-equation $\langle k\rangle$–$\langle\varepsilon\rangle$–$\langle\theta^2\rangle$ model for the parameterization of the unresolved (subscale) turbulence. Excellent agreement with experimental and DNS simulations of other authors have been obtained (Grötzbach, 1983; Wörner, 1994; Wörner and Grötzbach, 1995; Kerr, 1996; Kerr and Herring, 2000). In addition to accurate predictions of the integral and local heat transfer, the first and second-moments of turbulence quantities, very realistic representations of the unsteady behaviour of large convective structures have been obtained. In the present study, we extended the upper limit of Ra even further – up to 2×10^{16} observing clearly a tendency towards the Kraichnan (1962) ultimate regime for $Ra > 10^{13}$, Fig. 1(below). This regime is characterized by a change in slope of the integral heat transfer towards $Nu \propto Ra^{1/2}$ as also experimentally observed by Chavanne et al. (2001). It should be mentioned that even for the largest simulated values of Ra, a relatively modest grid was used with 128^3 CVs, though with a strong clustering in the near-wall region. For these high values of Ra, larger geometrical domains (8:8:1) are simulated. This is done in order to properly accommodate the elongated large-scale convective structures, which seem to acquire larger wavelengths with an increase in Ra, as shown in Kenjereš and Hanjalić (2000, 2002) and Hartlep et al. (2003). Again – as for smaller aspect ratios (4:4:1) – the free-slip boundary conditions are applied for all side boundaries. The key of success of T-RANS approach for accurate predictions lies in the anisotropic subscale representation of the second-moments which are dominant contributions in the near-wall region.

An important conclusion from this analysis emerged that the T-RANS with a subscale RANS-type model was fully adequate for this flow configuration without any need to change or to redefine the empirical coefficients evaluated in an extensive validation in a range of generic situations. The explanation for this success can be provided from the very nature of the problem. First, the natural forcing generated by the unsteadiness of the large convective structures that characterize thermal convection in configura-

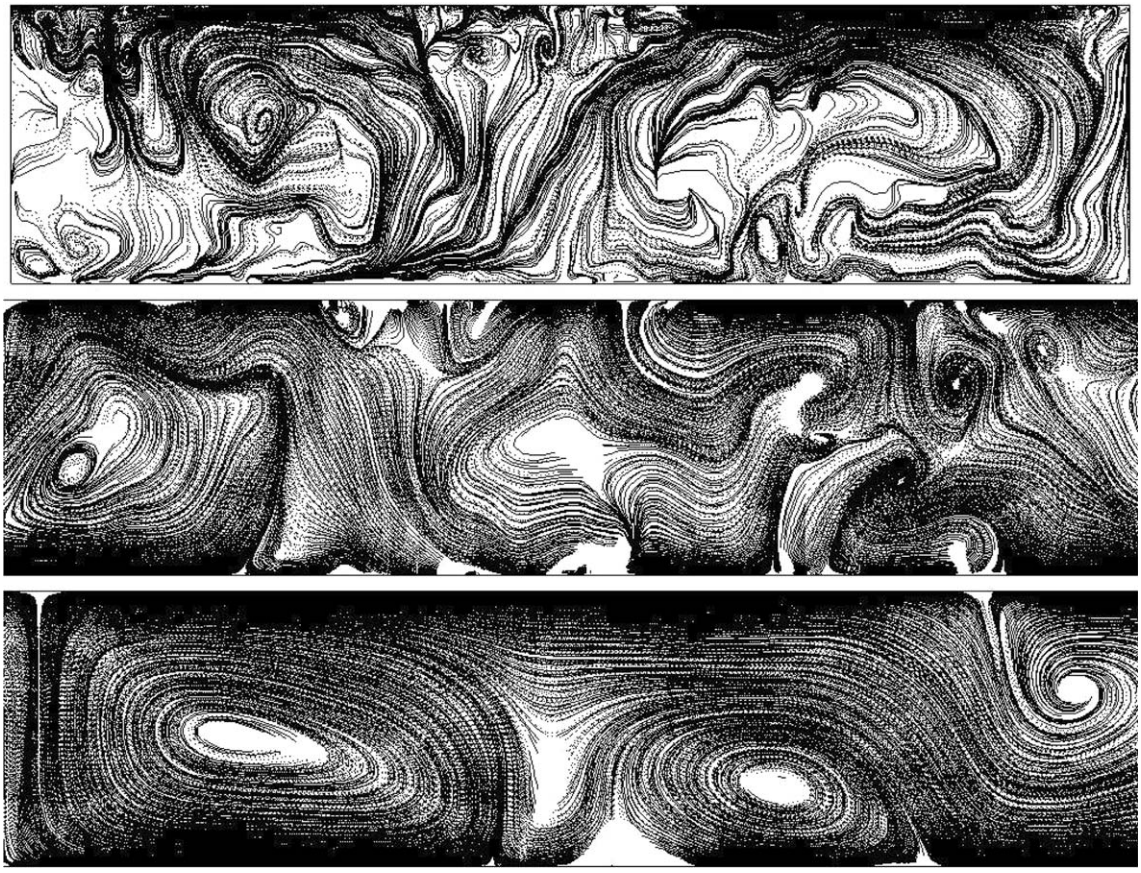

Fig. 7. Trajectories of massless particles of an instantaneous velocity field portraying the resolved flow structures in the central vertical plane. Above: well-resolved LES. Middle: HYBRID. Below: T-RANS approach; $Ra = 10^9$; please note that the T-RANS and HYBRID results are shown as a zoom-in of the 8:8:1 aspect ratio geometry.

tions heated from below (unstable thermal stratification), is so strong that the unsteadiness can be captured by simply applying unsteady computations, using any conventional RANS model for the subscale motion. The small-scale turbulence, produced in the near-wall region and in shear layers in rising plumes and convective rolls can be regarded almost as a passive scalar, with little or no effect on the large convective structures. On the other hand, close to the solid wall the fluid moves in a well established, though unsteady boundary layer, which is driven and perturbed by the unsteady large-scale convective roll/cell structures. Hence, despite interactions with the convective structures and eruption of plumes rising vertically and breaking the boundary layer, a near-wall RANS model tuned even in steady boundary layers in similar (buoyancy driven) flows seems sufficient to reproduce the averaged near-wall flow and turbulence statistics, including heat transfer.

The physical picture is quite different in the side-heated buoyancy driven flows. Here the turbulence is primarily located in the thin boundary layers and only weak interaction between the near-wall and central (weakly rotating or even stagnant) regions. In this case, the natural forcing is much weaker and it unlikely to expect that the transient-RANS approach will capture any natural unsteadiness. Our motivation is now to explore possibilities of sensitising the model to even weak natural unsteadiness, thus providing time resolution of at least very large coherent structures (very large-eddy simulations, VLES) in both vertical and horizontal generic configurations, thus being applicable to buoyancy driven flows irrespective of the heating orientation with respect to the gravitational vector.

The most obvious choice is to try to combine RANS and LES in a manner similar to the approaches used in the pressure driven flows, Dejoan and Schiestel (2001) and Hanjalić et al. (2004). For our applications, the hybrid "seamless" approach of Dejoan and Schiestel (2001) and Schiestel and Dejoan (2005) seems attractive since the above presented three-equations $\langle k\rangle$–$\langle\varepsilon\rangle$–$\langle\theta^2\rangle$ ASM/AFM model can be used to provide the eddy-viscosity for subscale turbulence over the complete flow domain. The major advantage of this method in comparison with the "zonal" hybrid strategy lies in its simplicity – it requires redefinition of only one empirical coefficient ($C_{\varepsilon 2}$). This coefficient is now expressed as a function of the ratio of the characteristic RANS and LES length scales. For $L_{\mathrm{RANS}}/L_{\mathrm{LES}} \leqslant 1$ range the RANS subscale model dominates and conventional T-RANS numerical method is active. For $L_{\mathrm{RANS}}/L_{\mathrm{LES}} > 1$, a reduction in $C_{\varepsilon 2}$ (towards $C_{\varepsilon 1}$) causes an increase in $\langle\varepsilon\rangle$ which in turn reduces the turbulent viscosity. Finally, for $C_{\varepsilon 2} = C_{\varepsilon 1}$, the DNS limit is reached. Additional appealing features are that this method does not require 'a priori' specification of the interface location and it does not exhibit discontinuities, as reported in hybrid methods with a demarcation (interface) between the RANS and LES regions.

In order to perform comparative assessment between different simulation approaches, the $Ra = 10^9$ case is selected. This value of Ra is large enough to be representative of highly turbulent thermal convection. The

Fig. 8. Trajectories of massless particles of an instantaneous velocity field portraying the resolved flow structures in the central horizontal plane ($z/H = 0.5$: above) and inside thermal boundary layer ($z/H = 10^{-3}$: below). Left: well-resolved LES. Middle: HYBRID. Right: T-RANS approach; $Ra = 10^9$.

well-resolved LES results (on $256^2 \times 128$ grid) are used as a reference for comparison. Simulations employing T-RANS, Hybrid and coarse-LES approach are run in parallel – but on a significantly coarser mesh with $82^2 \times 72$ CV, which represents just 5% of the total grid cells employed for fine LES. As a starting point in our analysis we recall that LES on this coarse mesh resulted in an underprediction of the integral heat transfer of 50%, Fig. 2(below). Our first goal is to reduce this enormous discrepancy to levels acceptable by industrial standards. The T-RANS approach resulted in excellent agreement with both experimental data of Niemela et al. (2000) and the fine-LES results. The long-term averaged vertical temperature profiles are shown in Fig. 3(above). It can be seen that the coarse LES shows huge discrepancy in the slope compared to fine-LES and T-RANS profiles. Different sets of parameters β^* and n for HYBRID approach have been tested in order to bring heat transfer prediction in good agreement with the fine-LES, Fig. 3(below). The strong damping of $C_{\varepsilon 2}$ coefficient in the RANS ($L_{\mathrm{RANS}}/L_{\mathrm{LES}} \leqslant 1 - \beta^* = 4$, $n = 2/3$) or buffer region ($1 \leqslant L_{\mathrm{RANS}}/L_{\mathrm{LES}} \leqslant 3 - \beta^* = 1$, $n = 8$) resulted in overall full suppression of the subscale turbulence quantities leading to quasi-DNS simulations. Proper behaviour of $C_{\varepsilon 2}$ should provide a two-way interactions between the near-wall and outer regions and this can be achieved by its gradual decrease. In the present study, the best results are obtained with $\beta^* = 1$ and $n = 2$, Figs. 2 and 3(below). The application of the wall-distance free variant of the model based on the α parameter resulted in very good agreement with the previous simulations but with significantly reduced empirical input and with encouraging potentials for applications in the complex geometries.

We focus our analysis now on the near-wall behaviour of the turbulence quantities – which are of primary importance

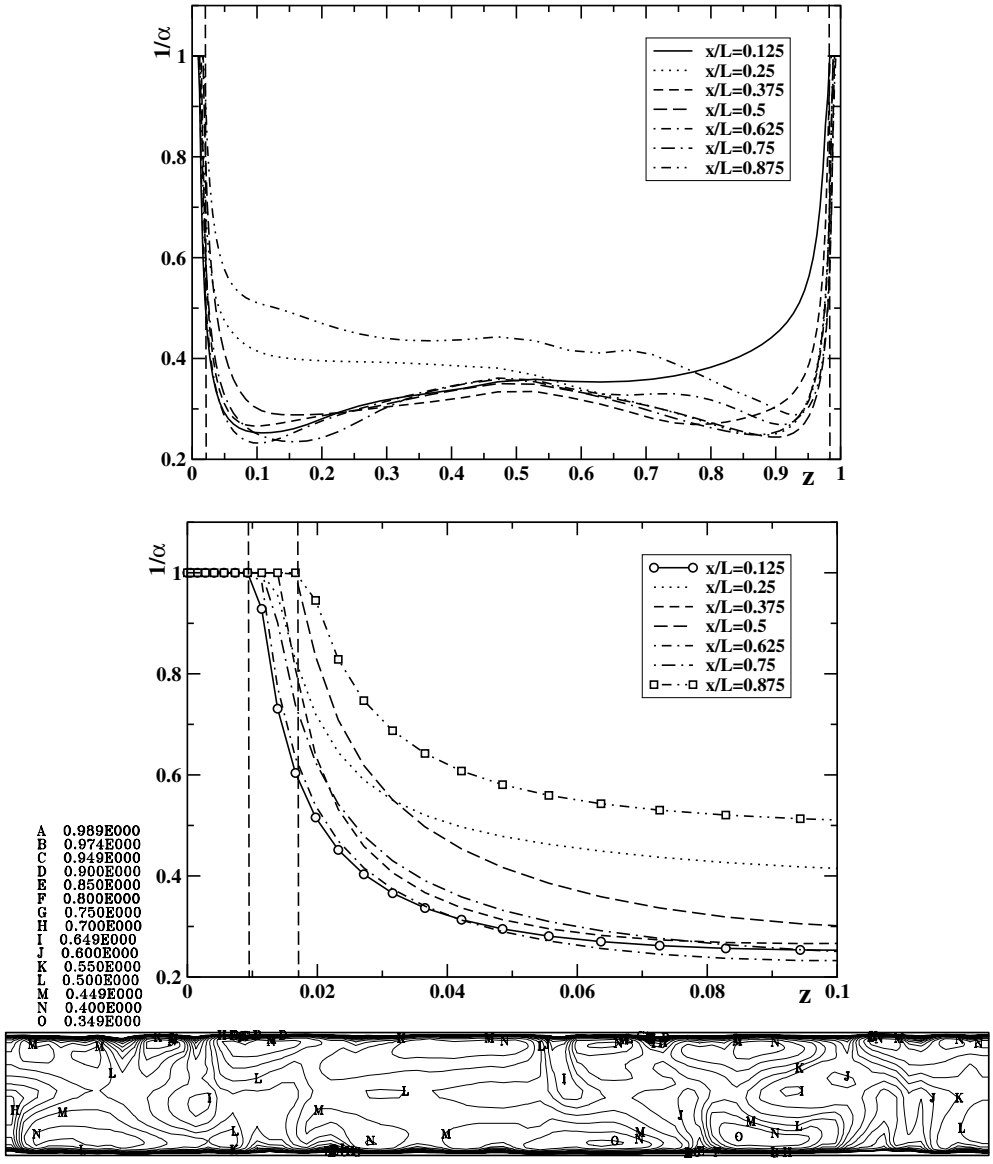

Fig. 9. Top: Vertical profiles of $1/\alpha$ at different locations along thermally active walls, $x/L = 0.0125, \ldots, 0.875$ for an arbitrary time realization. Middle: zoom in the near-wall region ($0 \leqslant z \leqslant 0.1$). Below: contours in the central vertical plane.

for accurate predictions of the wall friction and heat transfer, Figs. 4–6. The total contributions to heat flux, temperature variance and turbulence kinetic energy (divided in modelled and deterministic contributions) obtained by T-RANS and HYBRID approaches are compared with the fine-LES. The modelled contributions are obtained directly from their equations. The deterministic contributions are obtained from the triple-decomposition which assumes that an instantaneous property can be decomposed into time-mean, deterministic and random contributions, i.e., $\hat{\Phi}(x_i,t) = \overline{\Phi}(x_i) + \widetilde{\Phi}(x_i,t) + \phi(x_i,t) = \langle\Phi\rangle(x_i,t) + \phi(x_i,t)$. The long-term averaged deterministic contributions to the, e.g., heat flux can be expressed as $\overline{\widetilde{W}\widetilde{T}} = \overline{\langle W\rangle\langle T\rangle} - \overline{\langle W\rangle}\,\overline{\langle T\rangle}$ and $\overline{\widetilde{T}\widetilde{T}} = \overline{\langle T\rangle\langle T\rangle} - \overline{\langle T\rangle}\,\overline{\langle T\rangle}$. Generally, very good agreement between T-RANS, seamless hybrid and well-resolved LES is obtained for all considered variables. It is interesting to observe that the "seamless" approach shows an improvement in comparison with the T-RANS approach in the buffer region for all quantities. In addition, the hybrid approach reduced the modelled and increased the deterministic contribution. This change in redistribution is the consequence of significantly reduced turbulent viscosity in the outer region. Such reduced turbulent viscosity enables higher frequencies of the large-scale instabilities to be captured (as compared to the T-RANS approach). This is further illustrated by comparing the trajectories of massless particles in the central vertical and horizontal planes for the fine-LES, seamless hybrid and T-RANS, Figs. 7 and 8. It can be seen that the seamless hybrid approach captures a large portion of the smaller structures compared to T-RANS, as noted for the central vertical plane, Fig. 7(middle). Similarly, in the central horizontal plane, the vortical structures obtained by the hybrid approach show more intermittent behaviour compared with more regular T-RANS eddy structures, Fig. 8. This significantly enhances the model sensitivity to instabilities at higher frequency range, making the hybrid approach probably more suitable for the side-heated configurations compared to the T-RANS approach.

In order to illustrate which parts of flow domain are mainly affected by changing $C_{\varepsilon 2}$ – compared to standard T-RANS approach – profiles and contours of the $1/\alpha$ parameter are shown in Fig. 9. It can be seen that the proposed form of the hybrid RANS/LES approach allows dynamical adjustment (spatial and temporal dependence) of the parameter α – removing additional need to define a priori the interface region – as it is usually done in zonal hybrid RANS/LES approach. The full-RANS regions can be easily identified by clipping the areas where $1/\alpha$ is equal to one. These regions are located in proximity of the horizontal walls and represent approximately just 1% of the total distance between thermally active walls. In addition, it is important to note inhomogenities of these regions along the walls, Fig. 9(below). Different thickness can be observed indicating the self-adjusting features of the α parameter. All vertical profiles of the first- and second-moments (Figs. 3–6) exhibit a smooth transition between RANS and LES/DNS region proving "seamless" behaviour of the proposed approach.

5. Conclusions

A comparative assessment of different approaches to simulations of thermal convection over horizontal surfaces in turbulent regime is presented. In order to improve the potential of the conventional LES for accurate predictions of the near-wall heat transfer on moderately dense (RANS-type) grids, different variants of hybrid RANS/LES merging have been tested. It is demonstrated that the application of the T-RANS approach resulted in good agreement with the available DNS and fine-LES (for low *Ra*'s) and experimental results over a range of *Ra*. The key of success lies in modelling of the subscale turbulence contributions by the low-*Re* three-equation $\langle k\rangle$–$\langle\varepsilon\rangle$–$\langle\theta^2\rangle$ model which provides correct behaviour of turbulence variables in the near-wall region. In order to make the T-RANS approach capable of capturing the low-intensity flow instabilities and to capture unsteadiness also in flows with relatively weak forcing and broad turbulence spectrum – such as found in side-heated configurations – a simple redefinition of the modelled coefficient $C_{\varepsilon 2}$ (as a function of the RANS and LES turbulence length-scales ratio) is proposed. This "seamless" hybrid approach was then successfully applied to simulations of thermal convection at $Ra = 10^9$. Results show significant improvements in capturing of the smaller flow structures and slight improvements regarding the subscale turbulence variables in the buffer region. Especially encouraging are the results obtained with the wall-distance-free variant of the model based on the α parameter which has a potential especially for simulating flows in complex geometries.

Acknowledgements

The research of Dr. Saša Kenjereš has been made possible by a fellowship of the Royal Netherlands Academy of Arts and Sciences (KNAW). The access to supercomputing facilities at the SARA Computing and Networking Services in Amsterdam has been provided by the National Computing Facilities Foundation (NCF) and sponsored by the Nederlandse Organisatie voor Wetenschappelijk Onderzoek (NWO).

References

Castaing, B., Gunaratne, G., Heslot, F., Kadanoff, L., Libchaber, A., Thomae, S., Wu, X.Z., Zaleski, S., Zanetti, G., 1989. Scaling of hard thermal turbulence in Rayleigh–Bénard convection. J. Fluid Mech. 204, 1–30.

Chavanne, X., Castaing, B., Chabaud, B., Chanal, O., Chillá, F., Hébral, B., 1997. Free convection in low temperature gaseous helium. In: Hanjalić, K., Peeters, T.W.J. (Eds.), Proceedings of the 2nd International Symposium on Turbulence, Heat and Mass Transfer. Delft University Press, pp. 567–572.

Chavanne, X., Chilla, F., Chabaud, B., Castaing, B., Hebral, B., 2001. Turbulent Rayleigh–Bénard convection in gaseous and liquid He. Phys. Fluids 13 (5), 1300–1320.

Dejoan, A., Schiestel, R., 2001. Large-eddy simulations of non-equilibrium pulsed turbulent flow using transport equations subgrid scale model. In: Lindborg, E. et al. (Eds.), Turbulence and shear flow phenomena 2 (Proc. Int. Symp., Stockholm, Sweden, 27–29 June 2001) 2, pp. 341–346.

Eidson, T.M., 1985. Numerical simulation of the turbulent Rayleigh–Bénard problem using subgrid model. J. Fluid Mech. 158, 245–268.

Fleischer, A.S., Goldstein, R.J., 2002. High-Rayleigh-number convection of pressurized gases in a horizontal enclosure. J. Fluid Mech. 469, 1–12.

Grötzbach, G., 1983. Spatial resolution requirement for direct numerical simulation of Rayleigh–Bénard convection. J. Comput. Phys. 49, 241–264.

Hanjalić, K., 2005. Synergy of experiments and computer simulations in research of turbulent convection. Int. J. Heat Fluid Flow 26, 828–842.

Hanjalić, K., Kenjereš, S., 2001a. T-RANS simulation of deterministic eddy structure in flows driven by thermal buoyancy and Lorentz force. Flow, Turbulence Combust. 66, 427–451.

Hanjalić, K., Kenjereš, S., 2001b. VLES of flows driven by thermal buoyancy and magnetic fields (Chapter XII). In: Geurts, B.J. (Ed.), Modern Simulation Strategies for Turbulent Flow. R.T. Edwards Publishing, Philadelphia, PA, USA.

Hanjalić, K., Kenjereš, S., 2002a. Simulation and identification of deterministic structures in thermal and magnetic convection. Annals of the New York Academy of Sciences 972, Visualization and imaging in transport phenomena, pp. 19–28.

Hanjalić, K., Kenjereš, S., 2002b. Simulations of coherent eddy structures in buoyancy-driven flows with single-point turbulence closure models (Chapter XXII). In: Launder, B.E., Sandham, N.D. (Eds.), Closure Strategies for Turbulent and Transitional Flows. Cambridge University Press, UK, pp. 659–684.

Hanjalić, K., Hadžiabdić, M., Temmerman, L., Leschziner, M., 2004. Merging LES and RANS strategies: zonal or seamless coupling? In: Friedrich, R. et al. (Eds.), Direct and Large Eddy Simulations V. Kluwer Academic Publishers, pp. 451–464.

Hartlep, T., Tilgner, A., Busse, F.H., 2003. Large scale structures in Rayleigh–Bénard convection at high Rayleigh numbers. Phys. Rev. Lett. 91 (6), 1–4, 064501.

Kenjereš, S., Hanjalić, K., 1999. Transient analysis of Rayleigh–Bénard convection with a RANS model. Int. J. Heat Fluid Flow 20 (3), 329–340.

Kenjereš, S., Hanjalić, K., 2000. Convective rolls and heat transfer in finite-length Rayleigh–Bénard convection: a two-dimensional numerical study. Phys. Rev. E 62 (6), 7987–7998.

Kenjereš, S., Hanjalić, K., 2002. Numerical insight into flow structure in ultraturbulent thermal convection. Phys. Rev. E 66 (3), 1–5. Art. No. 036307, Part 2B.

Kerr, R.M., 1996. Rayleigh number scaling in numerical convection. J. Fluid Mech. 310, 139–179.

Kerr, R.M., Herring, J.R., 2000. Prandtl number dependence of Nusselt number in direct numerical simulations. J. Fluid Mech. 419, 325–344.

Kimmel, S.J., Domaradzki, J.A., 2000. Large eddy simulations of Rayleigh–Bénard convection using subgrid scale estimation model. Phys. Fluids 12 (1), 169–184.

Kraichnan, R.H., 1962. Turbulent thermal convection at arbitrary Prandtl number. Phys. Fluids 5, 1374–1389.

Niemela, J.J., Skrbek, L., Sreenivasan, K.R., Donnelly, R.J., 2000. Turbulent convection at very high Rayleigh numbers. Nature 404 (6780), 837–840.

Schiestel, R., Dejoan, A., 2005. Towards a new partially integrated transport model for coarse grid and unsteady flow simulations. Theor. Comput. Fluid Dyn. 18 (6), 443–468.

Smagorinsky, J., 1983. The beginnings of numerical weather prediction and general circulation modeling: early recollections. Adv. Geophys. 25, 3–23.

van Reeuwijk, M., Jonker, H., Hanjalić, K., submitted for publication. Direct numerical simulation of Rayleigh–Bénard convection at $Ra = 1.1 \times 10^8$.

Wong, V.C., Lilly, D.K., 1994. A comparison of two dynamical subgrid closure methods for turbulent thermal convection. Phys. Fluids 6 (2), 1016–1023.

Wu, X.Z., Libchaber, A., 1992. Scaling relations in thermal turbulence: the aspect ratio dependence. Phys. Rev. A 45, 842–845.

Wörner, M., 1994. Direkte simulation turbulenter Rayleigh–Bénard Konvektion in flüssigem Natrium. Dissertation, University of Karlsruhe, KfK 5228, Kernforschungszentrum Karlsruhe, Germany.

Wörner, M., Grötzbach, G., 1995. Modelling the molecular terms in the turbulent heat flux equation for natural convectionProceedings of the 10th Symposium on Turbulent Shear Flows, vol. 2. Pennsylvania State University, State College, USA, pp. 73–78.